AIRBORNE HYPERSPECTRAL AND THERMAL INFORMATION FOR ASSESSING THE HEAT ISLAND IN URBAN AREAS OF JAPAN

A.Ozawa, B. Babu Madhavan, H. Okada, K. K. Mishra, K.Tachibana and T.Sasagawa

GIS Institute, PASCO Corporation
1-1-2, Higashiyama, Meguro-ku, 153-0043, Tokyo, Japan
atsumasa_ozawa@pasco.co.jp

KEY WORDS: Hyperspectral, Thermal, High resolution, Urban, Aerial

ABSTRACT:

The heat island phenomenon, caused by urbanization, is one of the growing problems in Japan. In this study, we have described the radiometric temperature of the ground surface observed by the airborne thermal sensor in the Hiroshima City. The obtained results showed that the river and forest areas had lower temperatures whereas the roads had the highest. The temperatures of the Business District areas were almost same as that of the bare soils. We also observed the ground surface temperature in the Fuchu City, located near the Tokyo Metropolitan area and three kinds of hyperspectral responses of the several buildings were compared which were selected from the high, middle and low temperature buildings. We noticed the differences in the observed DN values. Finally we analysed the relationship between the reflectance and surface temperature of the same materials utilizing hyperspectral and thermal data. A negative correlation of the observed temperature in the daytime data was obtained, but no correlation was seen for the nighttime data. The study showed promising results for our current and future works to utilize the airborne thermal and hyperspectral sensing for assessing and mitigating the heat island in Japan.

1. INTRODUCTION

The heat island phenomenon, which is caused by urbanization, is one of the fast growing problems in Japan. However, few studies have been performed to observe the detailed surface temperatures by utilizing high resolution airborne remote sensing. Airborne observation is one of effective methods for the thermal mapping since it can cover large areas in a short time and capture the high-resolution data as well.

High reflective materials are one of the heat island reduction methods. They reduce temperature of the materials or sensible heat flux because incoming solar radiation energy is reduced by high reflection. We investigated the relationship between reflective intensity calculated by the airborne hyperspectral data and radiometric temperature of ground surface measured from the airborne thermal data for the three cities, Hiroshima (southern part), Osaka (central) and Tokyo (northern part), in Japan. As Hiroshima City in the recent years is experiencing an abnormal increase of the surface temperature due to the sprawling of the City, the necessity was highly realized to conduct the thermal mapping for the region.

Thermal properties of land-use/land-cover features were evaluated by airborne thermal images for the Hiroshima and Osaka Cities. We also attempted to assess the thermal properties along with hyperspectral data obtained for the Fuchu City in Tokyo areas.

2. URBAN HEAT ISLAND STUDY THROUGH REMOTELY SENSED DATA

Urban heat island (UHI) is a worldwide phenomenon in which urban areas absorb more heat than the suburban and rural areas. The phenomenon is primarily due to the alteration of urban landscape, which change the thermal response to solar radiation. The urban landscapes are characterized by an inability to reflect solar radiation. Dark-coloured objects such as buildings and streets, and less vegetation increase the ability of an urban landscape to store a lot of heat.

To appraise the effects of UHI, remotely sensed data have been used. Different approaches were established to analyse UHI by using the satellite derived surface temperature data. Surface temperature patterns for cities along mid-Atlantic coast were deduced from inferred from thermal infrared data of TIROS (Rao, 1972). Thermal data of NOAA AVHRR coupled with other satellite data have been used to evolve the relation between land-use/land-cover of urban and UHI (Carlson et al., 1977; Matson et al., 1978; Kidder and Wu, 1987; Brest, 1987; Balling and Brazel, 1988; Carnahan and Larson, 1990; Caselles et al., 1991, Babu Madhavan and Sachio Kubo, 1997). A good review on the utilization of satellite - derived surface temperature data for urban climate analyses was given in Gallo et al. (1995). The effects of UHI were educed by many evaluation studies of satellite derived vegetation index and radiant surface temperature (Gallo et al., 1993a; 1993b; 1995; Gallo and Tarpley, 1996).

The effect of UHI is not restricted to large cities. The effects have been detected in cities with populations of less than 10,000 people (Karl et al., 1988). Roth et al. (1989) estimated surface temperature data from NOAA AVHRR thermal infrared measurements and assessed its spatial distribution across several cities along the West coast of North America. In most of the UHI studies, higher surface temperatures were correlated to industrial areas and the vegetated areas to the cooler surface temperatures.

Albeit thermal infrared satellite data cannot directly accord the UHI effect, they can be studied with satellite-derived vegetation density measurements in an urban land use/land cover. The role of vegetation in reducing the amount of heat stored in the soil and surface structures due to transpiration, in contrast to relatively non-vegetated urban areas was analysed (Carlson et al., 1981;Goward, 1981; Goward et al., 1985; Goward and Hope, 1989). To estimate the amount of leaf area and related variables associated with agricultural crops (Gallo and Daughtry, 1987) as well as forests (Nemani and Running, 1989) vegetation indices have been computed from LANDSAT -TM, MSS, NOAA and SPOT data. To demonstrate the UHI effects, vegetation indices and radiant surface temperatures

acquired by AVHRR were correlated with minimum air temperatures observed for urban and rural locations (Gallo et al., 1993a, 1993b). The satellite-derived vegetation indexes (NDVI) were linearly related to the difference in observed urban and rural temperatures.

The thermal band (10.4-12.5 μm) of LANDSAT-TM has been used to measure the surface radiant temperatures (Malaret et al., 1985; Lathrop and Lillesand, 1987; Desjardins et al 1990). The look-up tables of Bartolucci and Mao Chang (1988) provide the users of LANDSAT-4 and LANDSAT-5 TM data to convert digital counts of the TM thermal band into temperature.

3. THERMAL IMAGING BY TABI SENSOR

We measured the radiometric temperature of the ground surface in detail by the airborne thermal sensor (Thermal Airborne Broadband Imager; TABI, manufactured by ITRES Research Ltd.). TABI-320 sensor available with PASCO Corporation has a pushbroom thermal imaging microbolometer, sensitive to the varied and changing thermal emissivity of the ground surface and creates geocorrected thermal image maps or mosaics. It consists of 320 spatial pixels and the sensor is integrated with GPS/IMU. Table 1 shows a brief specification of the TABI.

Field of view (FOV)	48°
Spectral range	8000 - 12000nm
Temperature range	-20 to 110°C (urban mode)
Thermal resolution	0.1°C

Table 1. Specification of the TABI

All substances emit the electromagnetic radiation having wavelengths ranging between 3000-14000nm. Each material has different emissivity, so we need to estimate accurate emissivity value to calculate the accurate temperature, however it's difficult to estimate it. In this study, we used emissivity value as 0.96, which is the fixed for the TABI.

Land surface temperature may be used to derive evaporation rates, or deduce other kinds of information from the surface temperature. Useful sensors are the sensors with bands in TIR, mainly 4100-4250 and 13000-15400nm. Recently PASCO Corporation has introduced TABI for the first time in Japan. Thermal images were collected over coastal and central parts of Japan covering Tokyo Bay and urban areas, Wakayama, Osaka, and Hiroshima Cities. Pilot studies were conducted over five places in Japan. TABI is capable of resolving temperature differences of 0.1℃ and lies between 8000 to 12000nm wavelength range. The sensor array has 320 microbolometer pixels. To understand the relationship of land-use patterns to heat production and its effect on the lowest layers in the atmosphere the remote sensing data can be used.

4. HYPERSPECTRAL IMAGING BY AISA SENSOR

PASCO Corporation owns AISA's Eagle (VNIR) and Hawk (SWIR) sensors (from the Spectral Imaging Ltd.). In the current study we used the Eagle, a pushbroom hyperspectral system integrated with GPS/IMU, that covers 400-970nm ranges, and variable up to 1024 spatial pixels. The high quality optics in the systems achieves practically nonexistent distortions. The Table 2 shows a general specification of the Eagle sensor.

Spectral Range	400 - 970 nm
FOV	39.7°, 29.9°, 63°
Spectral pixels	244
Spectral Resolution	2.9nm
GSD@1000m altitude	1.2m

Table 2. AISA's specification

5. RELATIONSHIP BETWEEN REFLECTANCE AND SURFACE TEMPERATURE

The Surface ground receives solar radiation energy and downward longwave radiation from the atmosphere or clouds. Received energy is emitted as upward longwave radiation, sensible heat flux, latent heat flux and ground heat flux (Figure 3). The following equation shows the relationship for the heat budget (Kondo, 1994),

$$R = \varepsilon \sigma Ts^4 + H + lE + G \qquad (2)$$

where, R = incoming radiation flux
Ts = ground surface temperature
H = sensible heat flux
LE = latent heat flux
G = ground heat flux
ε = emissivity
σ = Stefan-Boltzmann's constant

Incoming radiation flux can be described as,

$$R = (1\text{-ref})\, S - \varepsilon\, Ldown \qquad (3)$$

where, ref=reflectance
S=solar radiation energy
Ldown=downward longwave radiation

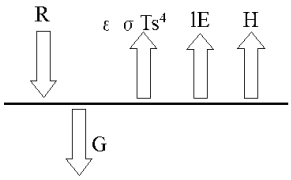

Figure 3. Heat Budget

In the case of the urban areas covered with concrete or asphalt, we can ignore latent heat flux because of the dry condition. Sensible heat flux depends on ground surface temperature. Equation (2) indicates that ground surface temperature depends on incoming radiation flux which is influenced by reflectance. So it will be expected that if reflectance increases, ground surface temperatures decrease.

The additional temperature in urban areas always has the damaging consequences of increasing demand for the electricity (for air conditioning) and increasing smog. Causes of the problem include the use of structural materials that are black in colour. The physics is simple that the materials are black because they absorb sunlight strongly. They can become very hot (as much as 21.11°C above the air temperature). The hot surfaces then heat the air, which causes discomfort. The chief culprits are dark roofs and asphalt pavements for the heat island.

The physics part of the work was to measure the reflectivity of conventional roofing and paving materials, and try to find

alternate materials that are more reflective. The surface temperature was also measured.

6. STUDY AREA AND DATA ANALYSIS

Thermal images were acquired over three Cities. The images of Hiroshima and Osaka areas were evaluated first. Hyperspectral images were captured for the Fuchu City of the Tokyo region.

6.1 Surface temperature of the Hiroshima City

Figure 4 shows the flight plan configuration and location of the Hiroshima City in Japan. There were eight EW flight courses with swath width of 960m/course. Figure 5 shows the thermal image of the Hiroshima City captured with ground spatial distance (GSD) of 3m from the flight altitude of 1078m on 9th September 2003 (between 17:00 to 18:00hrs). Surface temperatures observed by the TABI were modified by the measured data on the ground for the selected objects utilizing the handheld Raytek ST60 IR Non-Contact Thermometer covering the wavelength range of 8000 to 14000nm

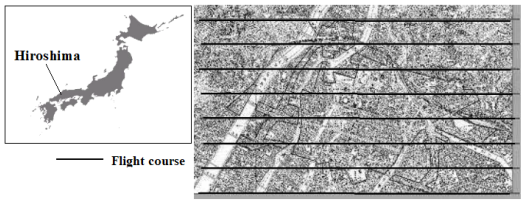

Figure 4. Observation area and flight courses in Hiroshima

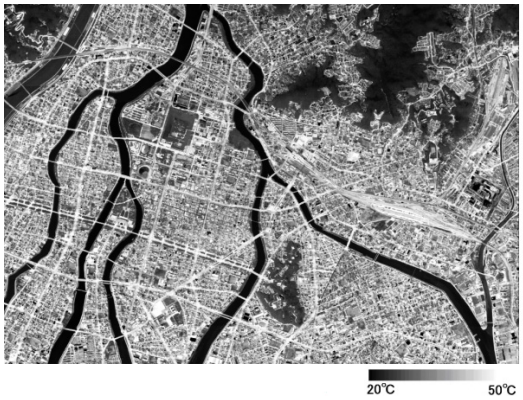

Figure 5. Thermal image of Hiroshima obtained from TABI

Table 6 shows the surface temperature of some areas selected from the thermal image as shown in Figure 5. River and forest temperatures are low and road temperature is the highest. The temperatures of the business districts showed almost same temperatures as that of the bare soil surfaces.

Area	Surface Temperature (°C)
River	28.0
Forest	28.4
Grass	30.1
Bare soil	34.1
Road (asphalt)	39.9
Business district	34.8

Table 6. Surface temperature of the land features

The castle area of the Osaka City with water as the heat sink feature was selected for the observation by TABI (Figure 7).

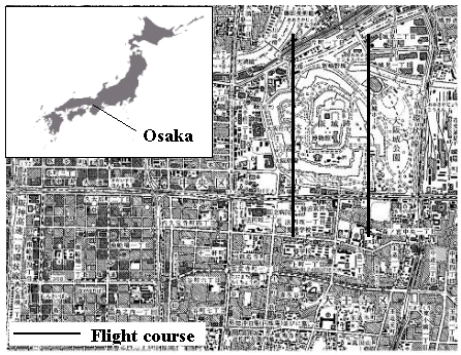

(a) Observation area and flight courses in Osaka City

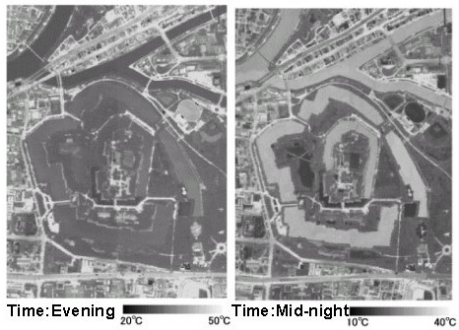

(b) Thermal images captured at two periods

Figure 7. Thermal image of Osaka City obtained from TABI

6.2 Comparison of hyperspectral data and surface temperature of building roofs

Figure 8 shows the thermal image of Fuchu City in Tokyo captured on 1st April 2004, GSD of 2m from the flight altitude of 730m. The ground surface temperatures were modified by the data of the simultaneous observation performed on same time with the ST60 IR Thermometer. In Figure 9 (a) the surface temperature of the black spots were lower than 15°C and white portions had higher than 36°C (the darker the pixel, the cooler the temperature).

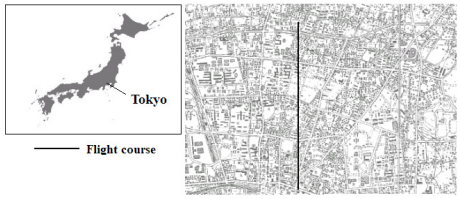

Figure 8. Observation area and flight courses in Fuchu City of Tokyo region

Figure 9 (b) is the hyperspectral data captured in 2003 and is displayed in the false colour combinations (bands 63, 30 and 5), in which vegetation is shown in red. It was observed from the thermal and hyperspectral data that the buildings and roads showed higher temperatures whereas vegetated and water areas indicated lower temperatures. It was noted that some buildings with temperature observations of lower than 15°C were caused by lower emissivity values.

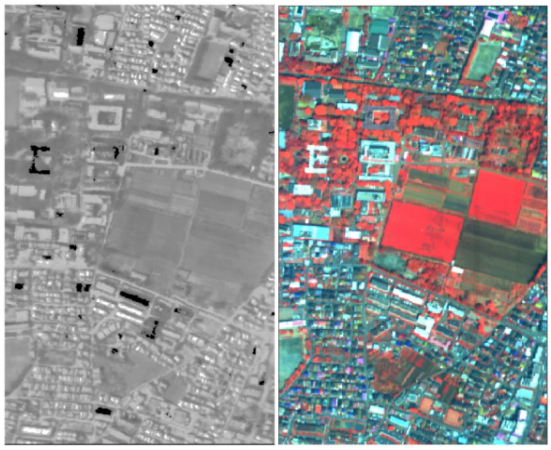

(a) (b)

Figure 9. Thermal (a) and hyperspectral (b) images of Fuchu

Figure 10 illustrates three kinds of spectrums generated from the hyperspectral data for several buildings, which were selected for the buildings of the higher temperature (higher than 36℃), middle temperature buildings (15℃to 36℃), lower temperature buildings (lower than 15℃). Although there is not much characteristic differences in the reflectance patterns, we noticed the differences in the digital number (DN) values (reflective intensity).

Figure 11 (a) describes the relationship between intensity of reflection estimated from the hyperspectral data and the temperature observed by the TABI. It indicated that the ground surface temperature became lower, as intensity of reflection became higher. We also analysed the airborne surface temperature data captured for the Osaka City. The observation was performed on 11th September 2003 at 16:45 and 14th September 2003 at 23:30hrs. The intensity of reflectance was estimated by the visible data (Red: 610-660nm, Green: 535-585nm, Blue: 430-490nm) and the NIR data (835-885nm) captured by airborne digital sensor (ADS40, GSD of 20cm) in August 2003, because the hyperspectral data was unavailable for that duration.

Values in Figure 11 (b) illustrate the relationship between intensity of reflection observed from ADS40 and ground surface temperature of the evening acquired by TABI. It indicates that ground surface temperature becomes low, as intensity of the reflection reaches higher values. Similarly, the plotted values in Figure 11 (c) shows the relationship between intensity of reflection (from the ADS40 image) and ground surface temperature in the midnight. It indicates that there is no relationship between the ground surface temperature and intensity of reflection. This was obviously because there was no solar radiation energy during the nighttime.

7. SUMMARY AND FUTURE WORK

We observed the surface temperature in Hiroshima City used by airborne sensor, 9th September 2003, between 17:00-18:00hrs. It showed that the road temperature was higher than river and forest temperature about 12°C. The surface temperatures of the business district areas had almost same temperatures as bare soils and higher than river and forest about 7°C.

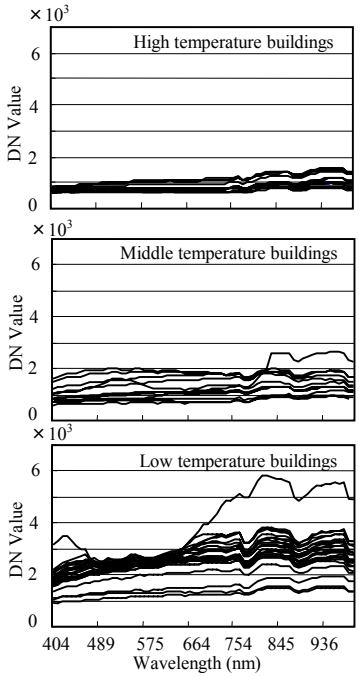

Figure 10. Differences in the spectrums by radiometric surface temperature

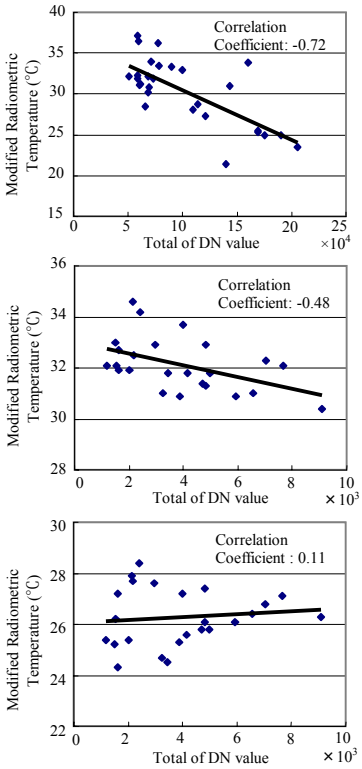

Figure 11. Relationship between reflectance and Ground surface temperature. (a) Fuchu City (b) Osaka City - evening time observations (c) Osaka City - midnight observations

After comparing the hyperspectral data with the temperature of the building-roofs, there were noticeable differences in the spectrum for the surface temperatures. There were not many characteristic differences in the reflectance patterns, but the differences were noticed for the DN values. The reflectance of the material between 400 to 970nm and surface temperature had the negative correlations. The present conducted study will

be helpful to provide valuable information and recommendations to the local agencies for assessing the UHI in the observed cities.

The future study will detect UHI phenomena, land use changed over specified periods of time. It will consider an interdisciplinary approach to explain the driving forces behind UHI effects; land-use and land-cover changes in the selected study sites. If all roofs were cooler the energy savings in many cities could be tens of millions of dollars a year. Lower temperatures would decrease the production of smog, which has many cities out of compliance with clean-air standards. Computer simulations will be carried out to estimate the citywide lowering of temperature and reduction of smog that deployment of whiter materials may achieve. The study also would develop a common protocol for methods and data sets, aimed at providing a framework for comparative studies. Policy related to urban planning such as urban forest development, roof garden reflective roof and road, transport planning etc. could be formulated. Effective mitigation methods can be suggested after finding the effects of UHI in the study areas.

REFERENCES

Babu Madhavan, B., and Sachio Kubo., 1997. Multi-sensor approaches to identify the effects of urban heat islands. In Proceedings of International Symposium on Monitoring and Management of Urban Heat Island, 19-20 November, Keio University, Japan, 220-241.

Balling, R.C., Jr., and Brazel, S.W., 1988. High Resolution surface temperature patterns in a complex urban terrain. Phot. Eng. Rem. Sens. 54:1289-1293.

Bartolucci and Mao Chang., 1988. Look-up tables to convert Landsat TM thermal IR data to water surface temperatures. Geocarto Int. 3:61-67.

Brest, C.L., 1987. Seasonal albedo of an urban/rural landscape from satellite observations. J. App. Meteo. 26:1169-1187.

Carnahan, W.H., and Larson, R.C., 1990. An analysis of urban heat sinks. Remote Sens. Environ. 33:65-71.

Carlson, T.N., Augustine, J.A., and Boland, F.E., 1977. Potential application of satellite temperature measurements in the analysis of land use over urban areas. Bulletin of the Am. Meteo. Soci. 58:1301-1303.

Carlson, T.N., Dodd, J.K., Benjamin, S.G., and Cooper, J.N., 1981. Satellite estimation of the surface energy balance, moisture availability and thermal inertia. J. Appl. Meteo. 20: 67-87.

Caselles, V., Lopez Garcia, M.J., Melia, J., and Perez Cueva, A.J., 1991. Analysis of heat-island effect of the city of Valencia, Spain, through air temperature transects and NOAA satellite data. Theo. Appl. Clima. 43:195-203.

Desjardins, R.,James Gray and Ferdinand Bonn., 1990. Atmospheric corrections for remotely sensed thermal data in a cool humid temperature zone. Int. J. Remote Sens. 11:1369-1389.

Gallo, K.P., and Daughtry, C.S.T., 1987. Differences in vegetation indices for simulated Landsat-5 MSS and TM, NOAA-9 AVHRR, and SPOT-1 sensor systems. Remote Sens. Environ., 23:439-452.

Gallo, K.P., McNab, A.L., Karl, T.R., Brown, J.F., Hood, J.J., and Tarpley, J.D., 1993a. The use of vegetation index for assessment of the urban heat island effect. Int. J. Remote Sens. 14:2223-2230.

Gallo, K.P., McNab, A.L., Karl, T.R., Brown, J.F., Hood, J.J. and Tarpley, J.D., 1993b. The use of NOAA AVHRR data for the assessment of the Urban Heat Island Effect. J. App. Meteo.. 32: 899-908.

Gallo, K.P., Tarpley, J.D., McNab, A.L., and Karl, T.R., 1995. Assessment of Urban heat islands: a satellite perspective. Atm. Res. 37:37-43.

Gallo, K.P., and Tarpley, J.D., 1996. The comparison of vegetation index and surface temperature composites for urban heat-island analysis. Int. J. Remote Sens. 17:3071-3076.

Goward, S.N., 1981. Thermal behaviour of urban landscapes and the urban heat island. Physical Geography, Remote Sens. Environ. 2:19-33.

Goward, S. N., Cruickshanks, G. D., and Hope, A. S., 1985. Observed relation between thermal emission and reflected spectral radiance of a complex vegetated landscape. Remote Sens. Environ. 18:137-146.

Goward, S. N., and Hope, A. S., 1989. Evapotranspiration from combined reflected solar and emitted terrestrial radiation: Preliminary FIFE results from AVHRR data. Adv. Space Res. 9:239-249.

Karl, T. R., Diaz, H.F., and Kukla, G., 1988. Urbanization: Its detection and effect in the United States climate record. J. Climate, 1:1099-1123.

Kidder, S.Q., and Wu, H., 1987. A multispectral study of the St. Louis area under snow-covered conditions using NOAA-AVHRR data. Remote Sens. Environ., 22:159-172.

Kondo, J., 1994. Meteorology for water environment, Asakura-shoten, 348pp.

Lathrop, R. G. and Lillesand, T. M., 1987. Calibration of Thematic Mapper thermal data for water surface temperature mapping:case study on the Great Lakes. . Remote Sens. Environ. 9:297-307.

Malaret, E., Bartolucci, L. A., Lozano, D. G., Anuta, P. E., and McGillem, C. D., 1985. Landsat-4 and Landsat-5 Thematic Mapper data quality analysis. Phot. Eng. Rem. Sens. 9:1407-1416.

Matson, M., McClain, E.P., McGinnis, D.F. Jr. and Pritchard, J.A., 1978. Satellite detection of urban heat islands. Monthly Weather Review, 106: 1725-1734.

Nemani, R.R., and Running , S. W., 1989. Estimation of regional surface resistance to evapotranspiration from NDVI and Thermal-IR AVHRR data. J. App. Meteo. 28: 276-284.

Rao, P.K., 1972. Remote sensing of Urban 'heat islands' from environmental satellite. Bull. Am. Meteo. 53: 647-648.

Roth, M., Oke, T.R., and Emery, W.J., 1989. Satellite-derived urban heat islands from three coastal cities and the utilization of such data in urban climatology. Int. J. Remote Sens. 10:1699-1720.